

OBSERVATION OF AEROSOLS FROM SPACE WITH THE AEOLUS MISSION

Alain Dabas⁽¹⁾, Vincent Lever⁽¹⁾, Pierre Flamant⁽²⁾

⁽¹⁾ Groupe d'Etude de l'Atmosphère Météorologique, Météo-France/CNRS, UMR3589, 42 avenue Coriolis, 31057 Toulouse cedex, France, Email : alain.dabas@meteo.fr

⁽²⁾ Laboratoire de Météorologie Dynamique, Ecole Polytechnique/CNRS, Ecole Polytechnique, 91128 Palaiseau cedex, France, Email : pierre.flamant@lmd.polytechnique.fr

ABSTRACT

The spaceborne Doppler lidar AEOLUS to be launched by ESA in 2015 will be the first high-spectral resolution lidar in space. By high-spectral-resolution, it is meant that the light backscattered by the atmosphere will pass through two interferometers, one large band, the other one narrow band. Provided the system is carefully calibrated, it is possible to measure independently the backscatter by the air molecules and the aerosols, and thus estimate both the backscatter and extinction coefficients of aerosols without making any prior assumption on the aerosol type. On the contrary, the independent estimation of both parameters not only characterizes the optical properties of aerosols – which is a valuable information for assessing the impact of aerosols on the energy balance of the atmosphere – but also give an indication on what type of aerosol is detected – dust, soot... AEOLUS should be of high value for all the scientific studies on the transport and modification of aerosols, but should also provide useful observations to the numerical models used for air quality predictions. The presentation will explain how AEOLUS can be used for observing aerosols and how the L2A processor designed for this purpose work.

1. INTRODUCTION

To be launched in mid-2015, AEOLUS is a Doppler lidar aimed at measuring winds over the globe and the entire depth of the atmosphere (up to about 25~30km). The lidar is designed and optimized for wind measurements. Winds are derived from the frequency Doppler shift between the emitted laser beam and the light reflected by molecules and particles. For wind measurements, the strength of the optical signal captured by the instrument is not used unless for computing their expected precision. However, the information is available and it can be used to detect aerosol plumes in the atmosphere and assess their optical properties.

Aerosols are a key factor of the energy balance of the atmosphere and presently constitute a major source of uncertainty. Depending on their chemical composition and size, aerosols have the capacity to absorb the solar light or the infrared radiation emitted by the earth. This is a direct impact of aerosols. But they also serve as

cloud condensation nuclei. Aerosols in larger numbers may produce a larger number of smaller water drops sharing the same amount of liquid water. This will have an impact on the cloud albedo (smaller cloud drops are more efficient in reflecting the solar light back to space) but will also affect the entire lifecycle of the cloud. Smaller drops may for instance inhibit rain and prolong the existence of the cloud.

Intensive research is conducted in order to improve the quality of aerosol simulation in climate and air quality models. For climate models, the objective is to be able to assess their net impact on the evolution of the energy balance of the atmosphere in the context of global warming. For air quality, the purpose is to be able to provide accurate predictions of the aerosol concentration.

Aerosol observations are already available from space, mainly from passive instruments. MODIS for instance provides maps of aerosol optical depths. The French-American CALIPSO lidar [1] brought information on their vertical distribution.

AEOLUS has the potential for extending the observation beyond CALIPSO. For this purpose, AEOLUS has an interesting capability: its receiver has two detection channels, one for the molecular backscatter, the other one for aerosols. Combining them, the molecular and aerosol contribution to the signal can be separated so that the aerosol backscatter and extinction coefficients can be derived. The provision of both parameters gives an indication of what type of aerosol is detected and thus gives a valuable information on where they are coming from (pollution, dust, ashes...).

2. LIDAR SIGNALS

The equation giving the strength of the lidar signal as a function of the distance z along the laser beam is

$$S(z) = \frac{K}{z^2} \beta(z) \exp\left(-2 \int_0^z \alpha(x) dx\right) \quad (1)$$

The coefficient K is an instrumental constant. The functions $\beta(z)$ and $\alpha(z)$ are the backscatter and extinction coefficients of the atmosphere. The backscatter β (in $m^{-1}sr^{-1}$) characterizes the capacity of the atmosphere to “reflect” the laser radiation back to

the lidar. The extinction coefficient α (in m^{-1}) characterizes the attenuation of the intensity of the laser beam along its propagation path. The attenuation can be due to scattering (photons scattered off the propagation axis are “lost”) or absorption.

Backscatter and extinction can be caused by molecules and particles. Therefore

$$\beta(z) = \beta_{aer}(z) + \beta_{mol}(z) \quad (2)$$

$$\alpha(z) = \alpha_{aer}(z) + \alpha_{mol}(z)$$

The molecular contributions β_{mol} and α_{mol} are known functions of the pressure P (in hPa), temperature T (in K) and laser wavelength λ (in nm)

$$\beta_{mol}(z) \cong 1.38 \left(\frac{550}{\lambda}\right)^{4.09} \frac{P(z)}{1013} \frac{288}{T(z)} 10^{-6} \quad (3)$$

$$\alpha_m(z) \cong 1.16 \left(\frac{550}{\lambda}\right)^{4.09} \frac{P(z)}{1013} \frac{288}{T(z)} 10^{-5}$$

Figure 1 shows both function as a function of the altitude for a standard atmosphere and the wavelength of AEOLUS $\lambda = 355nm$.

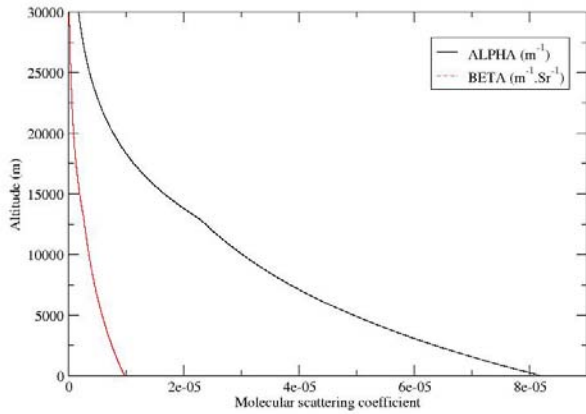


Figure 1 : Molecular extinction and backscatter as a function of the altitude for a standard atmosphere.

The aerosol backscatter and extinction are highly heterogeneous coefficients. Enhanced aerosol contents are generally found in the lowest hundreds of meters of the atmosphere in the so-called boundary layer. They are produced at the surface and lifted up by convection or turbulent eddies. Above the boundary layer, the aerosol concentration is generally much smaller except for possible payers of aerosols transported far away from their source by prevailing winds.

As it can be seen from Eq. (3), there is a well-defined relationship between α_{mol} and β_{mol}

$$\frac{\alpha_{mol}}{\beta_{mol}} = \frac{8\pi}{3} \quad (4)$$

There is no such simple solution for β_{aer} and α_{aer} . The ratio α_{aer}/β_{aer} is independent of the aerosol concentration (both parameters are proportional to the concentration), but depends on the nature and size

distribution of the aerosols. Figure 2 shows how this parameter varies with the aerosol type (from [2]). For urban/industrial aerosols for instance, the ratio is large because the aerosols are absorbing the light.

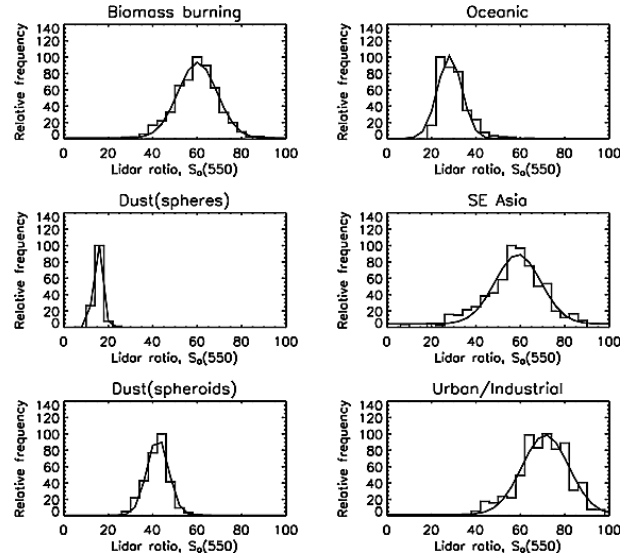


Figure 2 : Distributions of extinction to backscatter ratios for different types of aerosols (from [2]) and the wavelength $\lambda = 550nm$ (green).

People working observing the atmosphere with lidars would like to derive measurements for both α_{aer} and β_{aer} , but it cannot be done from a unique system as the signal is a combination of both parameters. The problem is mathematically ill-posed with one observation and two unknowns.

A common workaround is to assume the aerosol type is known (from an analysis of where prevailing winds are coming or from aerosol climatology) and postulate the value of the ratio α_{aer}/β_{aer} .

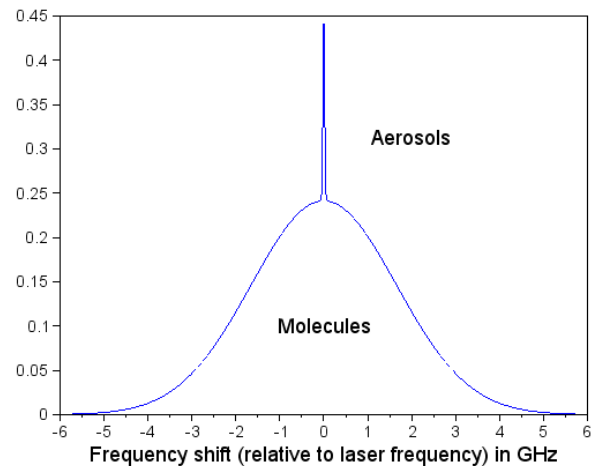


Figure 3 : Shape of the spectrum of a laser light backscattered by the atmosphere. The large part is caused by the molecules. The peak is due to the aerosols.

3. HIGH-SPECTRAL RESOLUTION

With AEOLUS, the a priori assumption is not necessary.

AEOLUS implements two detection channels. One is large band and is designed specifically for receiving the light backscattered by molecules. It is called the Rayleigh channel as a reference to Rayleigh theory. The second channel is narrowband and aimed detecting the light detected by particles with avoiding as much as possible the detection of molecular light. It is called the Mie channel as a reference to Gustav Mie who developed a theory for the scattering of light by spheres.

Figure 3 shows the typical shape of the light captured by the lidar. The wide part is nearly Gaussian. It is caused by molecules. At $\lambda = 355nm$, its FWHM is given by

$$\Delta\nu_{mol} = 224.8MHz * \sqrt{T(K)} \quad (5)$$

For $T = 300K$ for instance, we have $\Delta\nu_{mol} \approx 3.9GHz$. The peak is due to the scattering by particles. Its width is of the order of a few tens of MHz.

The Rayleigh and Mie channels are filtering the light. The filter characteristics of both are drawn in Figure 4 and Figure 5. The shape of the filter of the Rayleigh channel is due to the fact that the receiver implements two Fabry-Perot interferometric filters on either side of the spectrum. The Mie in the middle is thus partially filtered while a large part of the molecular spectrum goes through the filter. As for the Mie channel, it filters the spectrum in a narrow band of about the frequency of the emitted laser radiation.

It follows that the two signals recorded by the two channels can be written as

$$\begin{aligned} S_{Ray}(z) &= \frac{K_{Ray}}{R^2(z)} [C_1\beta_{mol}(z) + C_2\beta_{aer}] \exp\left(-2 \int_z^{+\infty} \alpha(x) dRx\right) \\ S_{Mie}(z) &= \frac{K_{Ray}}{R^2(z)} [C_3\beta_{aer}(z) + C_4\beta_{mol}] \exp\left(-2 \int_z^{+\infty} \alpha(x) dRx\right) \end{aligned} \quad (6)$$

where the coefficients C_1 to C_4 weight the relative contributions of aerosols and molecules to the two signals. Considering the passbands of Rayleigh and Mie filters

$$C_1 > C_2 \quad \text{and} \quad C_3 > C_4 \quad (7)$$

It follows the linear system in Eq. (6) is invertible so that the molecular and aerosol contributions can be separated

$$\begin{aligned} X_{mol}(z) &= \beta_{mol}(z) \exp\left(-2 \int_z^{+\infty} \alpha(x) dx\right) \\ X_{aer}(z) &= \beta_{aer}(z) \exp\left(-2 \int_z^{+\infty} \alpha(x) dx\right) \end{aligned} \quad (8)$$

Considering $\beta_{mol}(z)$ and $\alpha_{mol}(z)$ are known, the aerosol backscatter and extinctions can be easily derived

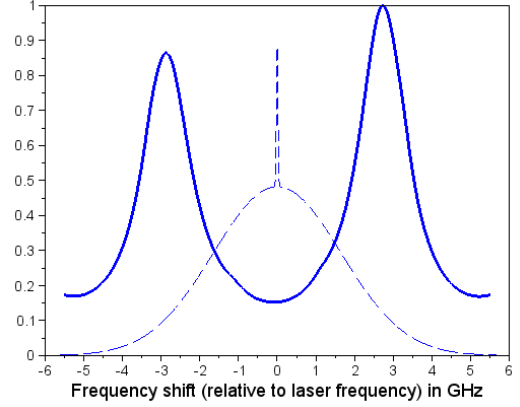


Figure 4 : Transmission characteristics of the broadband Rayleigh receiver.

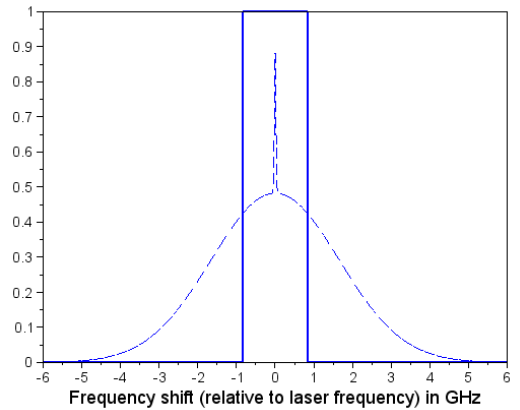


Figure 5 : Transmission characteristics of the narrowband Mie receiver.

$$\begin{aligned} \hat{\alpha}_{aer}(z) &= \frac{1}{2} \frac{d}{dz} \ln\left(\frac{X_{mol}(z)}{\beta_{mol}(z)}\right) - \alpha_{mol}(z) \\ \hat{\beta}_{aer}(z) &= \frac{X_{aer}(z)}{X_{mol}(z)} \beta_{mol}(z) \end{aligned} \quad (9)$$

4. L2A PROCESSOR

Eqs. (9) form the basis of the Level 2A processor of AEOLUS. Details can be found in [3]. It produces independent estimates for α_{aer} and β_{aer} wherever Mie and Rayleigh channel information is available.

The computation of X_{mol} and X_{aer} require a precise value for C_1 , C_2 , C_3 and C_4 . These coefficients are determined by a careful calibration of the system. For

C_1 and C_4 , the temperature, pressure and wind inside the sensed volume has to be known for their value depends on the shape of the molecular spectrum as well as its position relative to the transmission curve of the double Fabry-Perot Rayleigh receiver. The shape is described by Rayleigh-Brillouin theory of light scattering (see [4]). It is temperature and pressure dependent.

The needed meteorological information is provided by a numerical weather forecast. The sensitivity of C_1 and C_4 with respect to these parameters is weak so errors of several K , $10hPa$ or $10ms^{-1}$ can be tolerated. This is well within numerical weather prediction models reach.

In practice, S_{ray} and S_{mie} are integrated over vertical bins (see Figure 6). There are 24 Mie and 24 Rayleigh bins. Their thickness varies from 250m close to the ground to 2km at high altitudes. Perfect matching between Mie and Rayleigh bins is not possible – the top altitude of the topmost Rayleigh bin must be above the top altitude of the topmost Mie bin, but matching can be guaranteed for a large section of the atmosphere, making.

Due to the vertical bin-integration of Mie and Rayleigh signals; L2A products have a coarse and uneven vertical resolution. In particular, $\hat{\alpha}_{aer}$ and $\hat{\beta}_{aer}$ are vertical averages of $\alpha_{aer}(z)$ and $\beta_{aer}(z)$. The averaging kernel depends is a function of both parameters.

Figure 7 shows an example of vertical profile of backscatter retrieved by the L2A processor. The processor was applied to simulated lidar signals. The “true” backscatter field is shown on the top graph. There the backscatter is given as a function of height (y-axis) and measurement (x-axis). A measurement corresponds to the on-board horizontal integration of about 50 laser pulse returns. It defines the finest granularity of AEOLUS data. Two particle layers are visible: one at an altitude of about 5km, the second one at about 15km. Although the scene is heterogeneous; the L2A processor manages to retrieve a good profile (see red line in bottom graph, to be compared to the gray area that represents the average of the β_{aer} .

In addition to the retrieval of $\hat{\alpha}_{aer}$ and $\hat{\beta}_{aer}$, the L2A adds other functionalities like a feature finder (detection of atmospheric feature like clouds) and a scene classifier (distinction between aerosols, cloud of ice crystals, cloud of liquid water drops...).

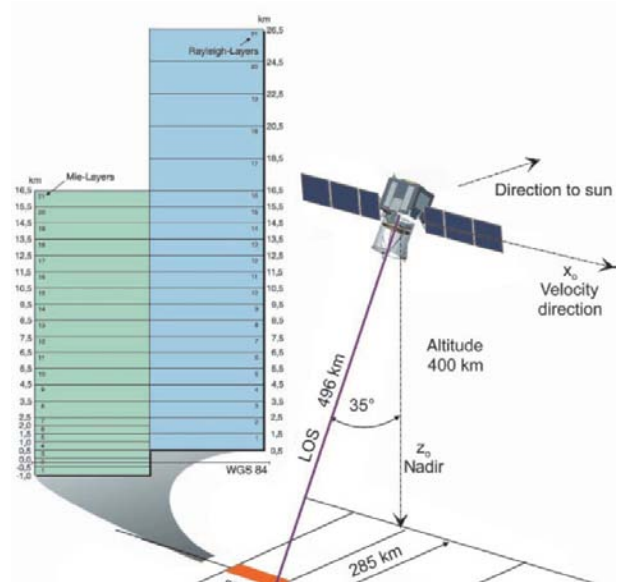


Figure 6 : Observation geometry of AEOLUS and Mie and Rayleigh height-bins.

REFERENCES

1. David M. Winker, Mark A. Vaughan, Ali Omar, Yongxiang Hu, Kathleen A. Powell, Zhaoyan Liu, William H. Hunt, Stuart A. Young (2009). Overview of the CALIPSO Mission and CALIOP Data Processing Algorithms. *Journal of Atmospheric and Oceanic Technology*, **26**(11), 2310-2323.
2. Christopher Catrall, John Reagan, Kurt Thome, Oleg Dubovik (2005). Variability of aerosol and spectral lidar and backscatter and extinction ratios of key aerosol types derived from selected Aerosol Robotic Network locations. *Journal of Geophysical Research*. **110**(D10S11), doi: 10.1029/2004JD005124.
3. Pierre H. Flamant, Juan Cuesta, Marie-Laure Denneulin, Alain Dabas, Dorit Huber (2008). ADM-Aeolus retrieval algorithms for aerosol and cloud products, *Tellus*, **60A**, 273-286.
4. Benjamin Witschas (2011). Analytical model for Rayleigh-Brillouin line shapes in air. *Applied Optics*, **50**(3), 267-270.

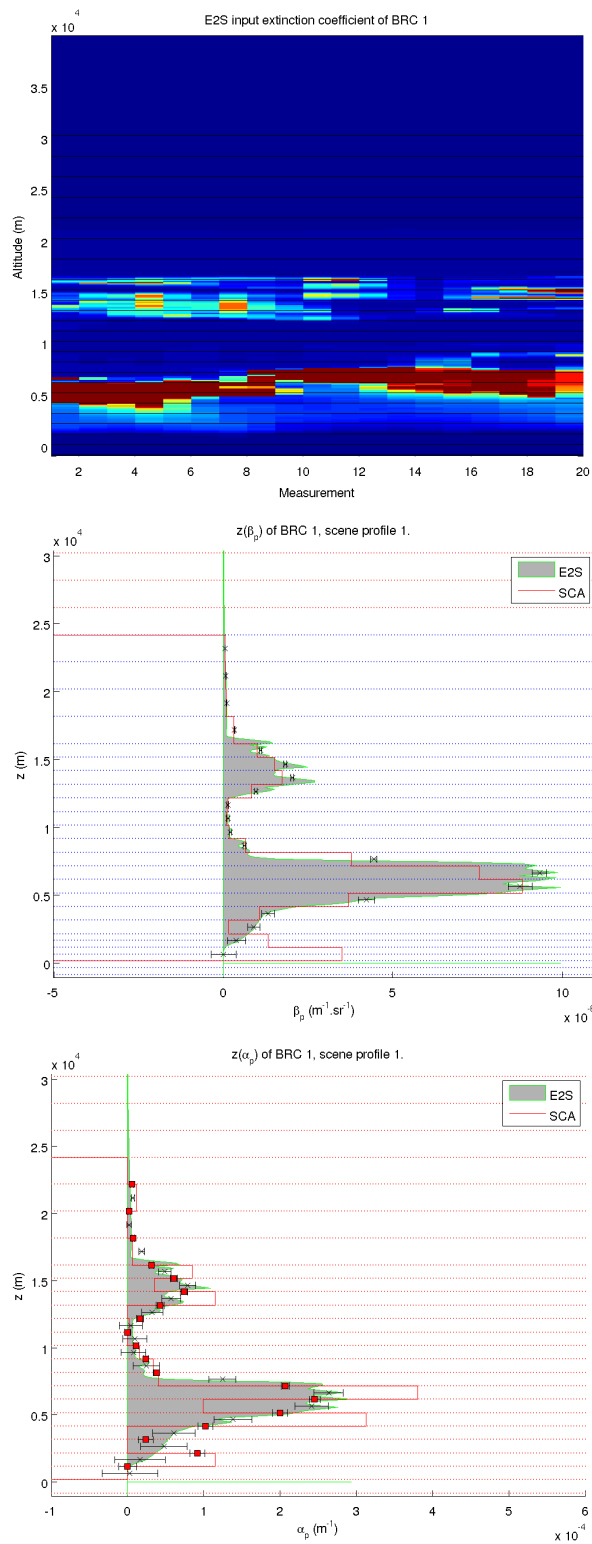


Figure 7 : Aerosol backscatter (middle) and extinction (bottom) retrieved by the L2A processor from lidar data simulated from the atmospheric scene shown on the top graph). There the extinction field is given as a function of the measurement number (a measurement is the on-board integration of Mie and Rayleigh signals produced by ~50 lidar shots). The grey shades are the average extinction and backscatter across the 20 measurements. The L2A retrieval is shown with a red line.